Thermal characterizations and investigation of the drawing region in Ge-As-S glasses for IR optical fibers

Matthieu Chazot, Mohammed El Amraoui, Steeve Morency, Anouar Hanafi, Younès Messaddeq, Vincent Rodriguez

Thermal characterizations and investigation of the drawing region in Ge-As-S glasses for IR optical fibers

Matthieu Chazot[1,2], Mohammed El Amraoui[2], Steeve Morency[2]
Anouar Hanafi[2], Younès Messaddeq[2], Vincent Rodriguez[1]

[1]*Université de Bordeaux, Institut des Sciences Moléculaires, CNRS UMR 5255, 351 cours de la libération, 33405 Talence cedex, FRANCE.*

[2]*Center for Optics, Photonics, and Lasers (COPL), Université Laval, Québec G1V 0A6, Canada*

Abstract

Several glass compositions of the Ge-As-S ternary system were prepared and their thermal and physical properties were investigated as T_g, T_d, theoretical drawing temperature T_s, viscous flow activation energy, density, visible and IR absorption coefficients. The measured values, which are in excellent agreement with the literature, were used to explore the drawing capability of the glass samples. In this work, we report wide range of Ge-As-S optical fiber compositions using the classical preform-to-fiber drawing technique. We show the possibility to obtain optical fibers with sulfur concentration ranging from 35 to 75%, and germanium concentration as high as 35%. In addition, based on the drawing tests we present a fiber drawing domain in the Ge-As-S ternary diagram. The attenuation losses measured at 1310 nm wavelength were between 8.4 and 12.3 dB/m.

Introduction

Since many years the need for optical fibers transmitting in the infrared range have attracted many research groups thanks to their potential of applications [1,2] as telecommunications, lasers sources, integrated optics, mid-infrared sensing for spectroscopy and defense [3]. Among the IR transmitting fibers, chalcogenide fibers present the highest transmission (up to 10 µm for sulfide, 20 µm for selenide and 30 µm for tellurium based glasses). The most known chalcogenide glass composition for optical fibers is indubitably the As_2S_3 for which is the lowest loss of 23 dB/km has been reached at 2.4 µm [4]. Still, the requirement of materials transmitting at higher wavelength or having higher nonlinear refractive index have led to the research of new chalcogenide fibers of various compositions (TeAsS, GeAsSeTe, SeSGaGe etc..). However each compositions suffer of specific limitations. We can cite for example lower T_g and transmission in the visible for Se or Te based glasses compared to sulfurs, but also smaller vitreous domains which can limits the choice of stoichiometry compositions and hence core/clad refractive index difference, etc. On the other hand, the extensive research on multimaterial fibers requires glass compositions and optical fibers with high flexibility in terms of T_g, drawing temperature, transmission window, refractive index, and glass compositions. For chalcogenide glasses, Ge-As-S is the ternary system having the widest glass forming region [5] which is very important in the choice of the glass composition depending on the application targets. Those glasses are also known for their properties regarding photo-induced anisotropy [6], and their thermal or structural properties have been well studied which is of interest when a structure-property correlation is needed [7,8]. Nevertheless, despite the large appealing of this system, there is a few number of publications discussing their fiber drawing ability [9,10]. Regarding this lack of information, we propose a study of the fiber drawing region within the glass forming region of the Ge-As-S system. In the present study, we will firstly explore the thermal and physical analysis of the glass sample before the drawing process. We performed thermomechanical analysis and viscosity measurements of all compositions over the vitreous

domain of Ge-As-S ternary system. Our main goal was to extract theoretical drawing temperatures and anticipate the evolution of viscosity as a function of temperature for the different glass compositions. Then, the second part will be dedicate to explore the drawing tests results and perform some fiber characterizations.

Experimental

1. Glass and preform fabrication:

The melt-quenching technique was used to prepare Ge-As-S glasses, starting from high purity elements, germanium (5N), arsenic (5N) and sulfur (7N). No additional steps of purifications were made for this study. The batches were introduced into a silica glass ampoule and sealed under high vacuum (10^{-5} Torr), forming closed synthesis tubes to avoid sulfur evaporation and arsenic sublimation during melting procedure. In the aim to avoid a fast increase of the pressure in the ampoule which could lead to its explosion, the synthesis were made using a slow heating ramp of 1°C/ min. It also contribute to the progressive reaction of the precursors until the furnace riches the final temperature of 850-900°C (depending on the composition of the glass). The rocking furnace was held at this temperature during 12 hours for the homogenization of the melt. Synthesis tubes has been quenched into water at 650°C, and annealed in a furnace at 10°C below the T_g for 6 hours. The samples were then gradually cooled to the room temperature in the aim to remove the internal stress. Preforms with 12 mm of diameter and 80 mm of length were obtained directly in the silica glass ampoules after quenching. Before drawing, glass pieces of 1-2 mm of thickness were cut from the preform and polished for optical characterizations.

2. Fiber drawing:

Single index optical fibers with diameter of 180-200 μm were obtained by the use of preform-to-fiber drawing technique [11,12], following the same experimental procedure describe elsewhere [13].

3. Material characterization:

Measurement of glass transition temperatures (T_g), dilatometric softening temperature (T_d) and linear thermal expansion coefficient (α) were recorded by thermomechanical analysis (TMA) using a Netzsch 402F1 Hyperion apparatus. Cylindrical samples of 8 mm diameter and 6 mm length were brought in contact with a silica pushing rod inside a furnace and heated at a rate of 5°C/min up to ± 20 °C besides the glass softening temperature. The relative variations of samples length as function of temperature were measured by a highly sensitive inductive displacement transducer via the push rod. The measurement accuracy for the linear expansion coefficient was ± 0.05 °C/min, and ± 2°C for T_g and T_d. Viscosity measurement were made by using a Bansbach Easylift Theta US parallel plate Viscosimeter on samples having the same geometry than those prepared for the TMA analysis. The samples were introduced between two silica discs and placed in contact with a silica rod connected to a linearly variable differential transformer (LVDT) which allow to record the thickness variation rate of the samples as function of time. The samples were heated at a rate of 2°C/ min up to the final temperature for which the viscosity value of $10^{7.5}$ Poises was reached under a compressive charge load of 300 g. For better precision the measurements were performed twice for each glass composition and the estimated error for the temperature was about ± 3°C and for the viscosity was $10^{\pm 0.2}$ Poises. After synthesis, the stoichiometry of the different glass composition was controlled using a CAMECA-SX100 electron probe micro-analyzer (Cameca, Gennevilliers, France). The measurements were made by wavelength-dispersive spectroscopy (WDS) using an electron microprobe (EPMA), applying a current of 20 nA and an accelerating voltage of 15 kV. Infrared (IR) absorption spectra were recorded employing a

PerkinElmer Frontier FTIR, with a resolution of 4 cm^{-1} and 16 accumulations. Infrared absorption spectra were normalized by the thickness of the samples which were measured using a mechanical profilometer with a ± 2µm of precision. Fiber loss attenuations measurements were done on 2 meters fiber length, by using the classical cut-back technique on two different set-ups. The first set-up is the same as the one used in ref. [13], where the selected light emerging from two available sources emitting at 1310 and 1550 nm was lunch into the fiber using a 20 X objective with 0.32 numerical aperture NA. A three axis sample stage was used to adjust the fiber position at the injection, and the end of the fiber was directly placed onto the surface of a thermopile detector (GENTEC) to measure signal transmitted through the fiber (accuracy measurement 0.1dB/m). For the second set-up a mid-infrared supercontinuum laser (Targazh) emitting between 1.5 and 4.3 µm combined with a monochromator (Bruker) and a PbSe detector were used to measure the attenuation loss. Cleaves quality were checked by an optical microscope.

Results and discussion

Bulk glasses

In the aim to get a better understanding of the different glasses before making drawing tests physical and thermal analysis have been made. The operating range of the viscometer is around $10^{9.5}$ and $10^{7.5}$ Poises, and it is important to know the appropriate starting temperature. Since the glass softening temperature correspond to a viscosity of $10^{9.5}$ Poises, we performed thermomechanical analysis measurement to obtained the value of T_d and then to be able to make viscosity measurements. Figure 1 shows the TMA curves of Ge-As-S glasses along the $(GeS_2)_x$—$(As_2S_3)_{100-x}$ composition line. From the obtained curves we were able to extract the dilatometric glass transition temperature as well as the dilatometric softening

temperature and the thermal expansion coefficient of each sample. Figure.1 shows the increase of T_g and T_d values through the increase of germanium concentration and the opposite was observed for thermal expansion coefficient. Those observations are in accordance with the fact that germanium is fourfold coordinated while arsenic is threefold coordinated. Thus replacing arsenic by germanium will increase the network reticulation which will decrease the thermal expansion coefficient. Moreover the bond dissociation energy of Ge-S (534 ± 3 $kJ.mol^{-1}$) is comparatively higher than As-S (379.5 ± 6.3 $kJ.mol^{-1}$) [14] which explain the raise of T_g and T_d and the decrease of α when the Ge content increase.

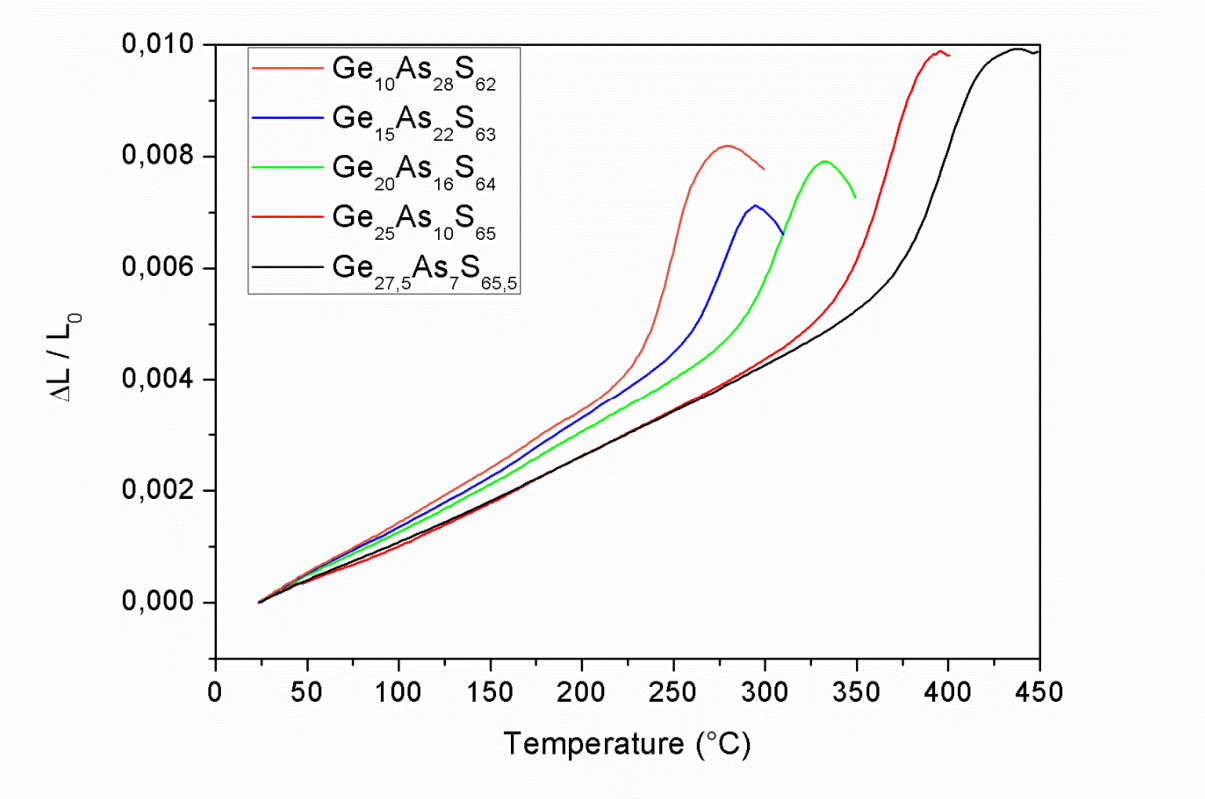

Figure 1: Thermomechanical analysis of Ge-As-S glasses according to the composition line $(GeS_2)_x—(As_2S_3)_{100-x}$

Figure 2.a shows the evolution of viscosity as a function of germanium concentration along the $(GeS_2)_x—(As_2S_3)_{100-x}$ composition line. One can observe the temperature increase for a given value of

log (η) when Ge content increase. As in the case of T_g and T_d this increase is due to the higher bond dissociation energy of Ge-S compare to those of As-S. In the same time we can see an increase in the slope of the viscosity curves with the increase of germanium concentration, which leads to the rise of the flow activation energy following the viscosity equation:

$$\eta = \eta_0 e^{\frac{\Delta H_\eta}{RT}} \quad (1)$$

Where η is the viscosity, η_0 is the pre-exponential factor, R is the gas constant, T is the temperature and ΔH_η is the viscous flow activation energy. Hence, from the log (η) plots as a function of 1/T, one can extract the values of ΔH_η for each glass sample which are proportional to a slope of a linear curve. Even if this mathematical treatment of the viscosity can lead to an overestimation of the viscous flow activation energy [15], the comparative evolution of the values allow us to have some information. For instance the increase of ΔH_η with Ge content is of particular interest as it results in a more pronounced evolution of viscosity in the same range of temperature. Consequently, smaller steps will be required when we will increase the temperature of the glass during drawing tests. Figure 2.b shows the evolution of viscosity as a function of sulfur content for glasses having Ge/As ratio close to 1.25 (arbitrary choice). We can clearly observe an increase of the temperature for the same viscosity value as well as a rise of the slope and therefore ΔH_η when sulfur content decrease. Indeed, by increasing the metalloids content we increase the network reticulation and therefore the energy needed to dissociate the bonds. This conduct to an augmentation of the energy required to enable flow of the liquid. From viscosity curves we were also able to evaluate the values of theoretical drawing viscosity T_s for the samples (viscosity ranging between $10^{5.5}$ and $10^{6.5}$), using a linear plot of the curves. Those information allowed us to start the drawing tests directly to a temperature around to the theoretical drawing temperature and thereafter avoid crystallizations of the preforms during heat treatment.

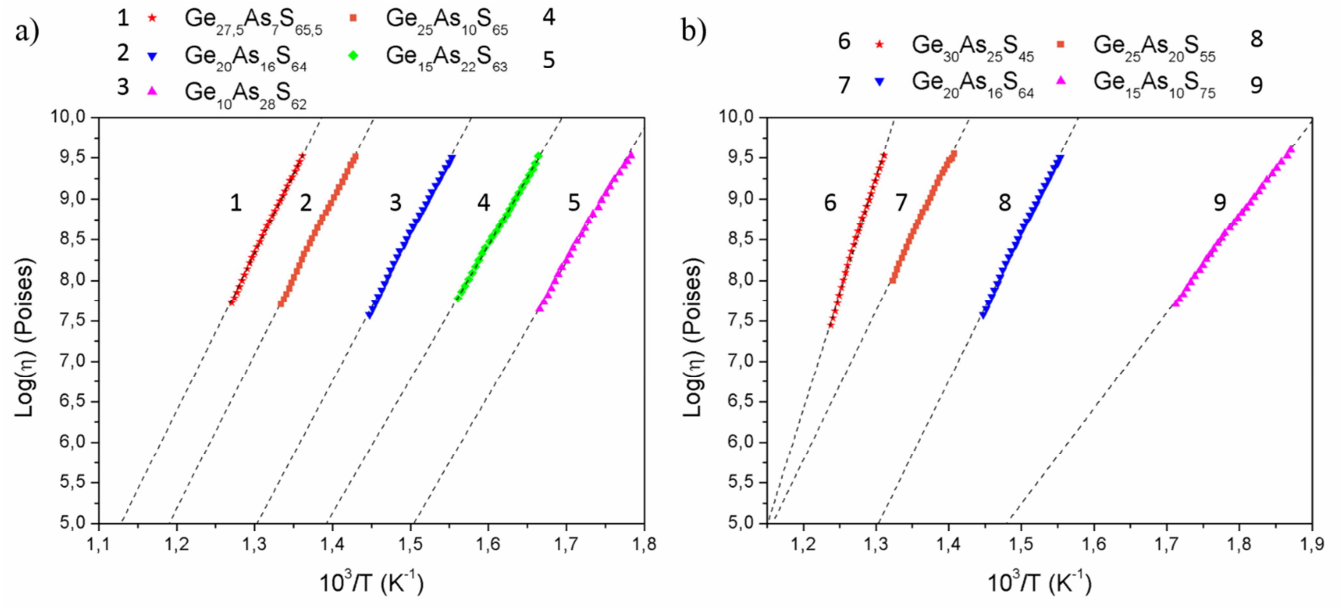

Figure 2: Viscosity curve as a function of the inverse of temperature for a) $(GeS_2)_x$—$(As_2S_3)_{100-x}$ glasses and b) Ge-As-S glasses having Ge/As ratio around 1.25.

The results obtained for all the samples are reported on Table 1. The results show an excellent agreement with the data published by B.G. Aitken and C.W. Ponader [8]. Still, some data are missing for two compositions, namely $Ge_{40}As_{25}S_{35}$ and $Ge_{15}As_{30}S_{55}$. For the first one TMA measurement was impossible to exploit due to an important curve fluctuations, which are probably relied to the beginning of crystallizations. This was not critical for viscosity measurement but the measured values might be strongly affected and should be taken with special care. For the second, we observed a huge crystallization of the sample during the viscosity measurement and no viscosity values have been extracted. Likewise, one can note the unusually high value of expansion coefficient (α) that has also been observed by B.G. Aitken and C.W. Ponader [8], which is relied to the presence of As_4S_3 molecular units in the glass samples [5].

Table 1: Glass transition temperature (T_g), dilatometric softening temperature (T_d), theoretical drawing temperature (T_s), density, thermal expansion coefficient and viscosity activation energy, mean coordination number MCN (see Eq. 1), and Ge/As ratio of Ge-As-S glasses.

Glass compositions	T_g (°C) ± 2	T_d (°C) ± 2	T_s (°C) ± 2	Density ($g.cm^{-3}$) ± 0.001	α (10^{-6} K^{-1}) ± 0.05	ΔHη ($kJ.mol^{-1}$)	MCN	Ge/As ratio
$Ge_{20}As_{45}S_{35}$	370	410	518-547	3.73	11.744	423.15	2.85	0.44
$Ge_{32.5}As_{32.5}S_{35}$	430	462	564-587	3.818	9.501	603.46	2.975	1
$Ge_{40}As_{25}S_{35}$	435	-	540-559	3.919	-	704.77	3.05	1.6
$Ge_{20}As_{35}S_{45}$	335	376	504-535	3.417	14.472	373.64	2.75	0.57
$Ge_{25}As_{30}S_{45}$	381	429	539-568	3.449	13.35	449.71	2.8	0.83
$Ge_{30}As_{25}S_{45}$	415	458	558-583	3.46	11.078	546.46	2.85	1.2
$Ge_{35}As_{20}S_{45}$	435	455	545-566	3.51	10.277	636.01	2.9	1.75
$Ge_{15}As_{30}S_{55}$	264	314	-	3.123	46.97	-	2.6	0.5
$Ge_{20}As_{25}S_{55}$	307	398	476-509	3.133	23.247	336.28	2.65	0.8
$Ge_{25}As_{20}S_{55}$	360	418	534-571	3.132	12.91	352.56	2.7	1.25
$Ge_{30}As_{15}S_{55}$	415	486	563-592	3.121	13.642	481.76	2.75	2
$Ge_{28}As_{12}S_{60}$	391	448	551-585	2.979	13.578	397.67	2.68	2.33
$Ge_{10}As_{28}S_{62}$	233	279	354-379	3.061	20.422	316.12	2.48	0.36
$Ge_{15}As_{22}S_{63}$	260	295	401-430	3.004	20.7	316.46	2.52	0.68
$Ge_{20}As_{16}S_{64}$	270	332	448-478	2.95	18.849	347.9	2.56	1.25
$Ge_{25}As_{10}S_{65}$	353	395	515-550	2.882	17.411	363.52	2.6	2.5
$Ge_{27.5}As_{7}S_{65.5}$	380	438	557-595	2.848	16.49	371.57	2.62	3.93
$Ge_{26.12}As_{6.65}S_{67.23}$	335	390	520-557	2.818	16.3	336.41	2.58	3.93
$Ge_{28.87}As_{7.35}S_{63.78}$	390	435	568-603	2.879	15.24	404.85	2.65	3.93
$Ge_{10}As_{15}S_{75}$	146 - 155	203	302-334	2.666	15.647	217.89	2.35	0.67
$Ge_{15}As_{10}S_{75}$	160 - 168	260	349-383	2.654	30.259	225.76	2.4	1.5

We also reported on Table 1 the mean coordination number (MCN) of the samples, introduced by Phillips and Thorpe [16,17], as well as the Ge/As ratio. The MCN is the average coordination number per atom and is expressed as follow:

$$MCN = 4x + 3y + 2z \quad (2)$$

Where x, y and z are the atomic percent of germanium, arsenic and sulfur respectively. The MCN values give a measure of the 3-D glass network connectivity, taking into account that germanium is fourfold coordinated, arsenide threefold and sulfur twofold coordinated. I has been showed by Phillips and Thorpe [16,17] that chalcogenide glass compositions with MCN value equal to 2.4 correspond to an ideally constrained network and were more favorable for glass formation. For instance a correlation can be made between the raise of T_g and T_d and the augmentation of the MCN values for the glass samples along the $(GeS_2)_x$—$(As_2S_3)_{100-x}$ composition line when GeS_2 content increase. As discussed before the increment of germanium in the system increase the network reticulation, which is illustrated by an increase of the MCN value. In the same time for a Ge/As constant ratio we can observe an increase of the MCN when the sulfur content decrease, which leads to an increase of T_g and T_d. Managing the Ge/As ratio is also important, because in this ternary system one can count two different metalloid elements. Due to the fact that they have distinctive coordination numbers and structural characteristics, they will influence differently the glass properties.

Knowing the optical transparency range of a glass is important for optical fiber applications. Indeed, as can be seen on Figure 3, using germanium instead of arsenic leads to a diminution of the low wavelength glass cutoff *i.e* diminution of the band-gap. This is due to the fact that the GeS_2 has a higher band-gap (E_g = 3.42 eV) [18] compared to theAs_2S_3 (E_g = 2.34 eV) [19]. Commonly, GeS_2 glasses are known to be yellow whereas As_2S_3 glasses are red. Then, on the shot of the samples in Figure 3, we observe a progressive change in color along the $(GeS_2)_x$—$(As_2S_3)_{100-x}$ composition line from yellow

(compositions close to GeS_2) to red (compositions close to As_2S_3). The glass labelled C appeared to be darker on the picture due to the light scattering of syrups presence in the glass.

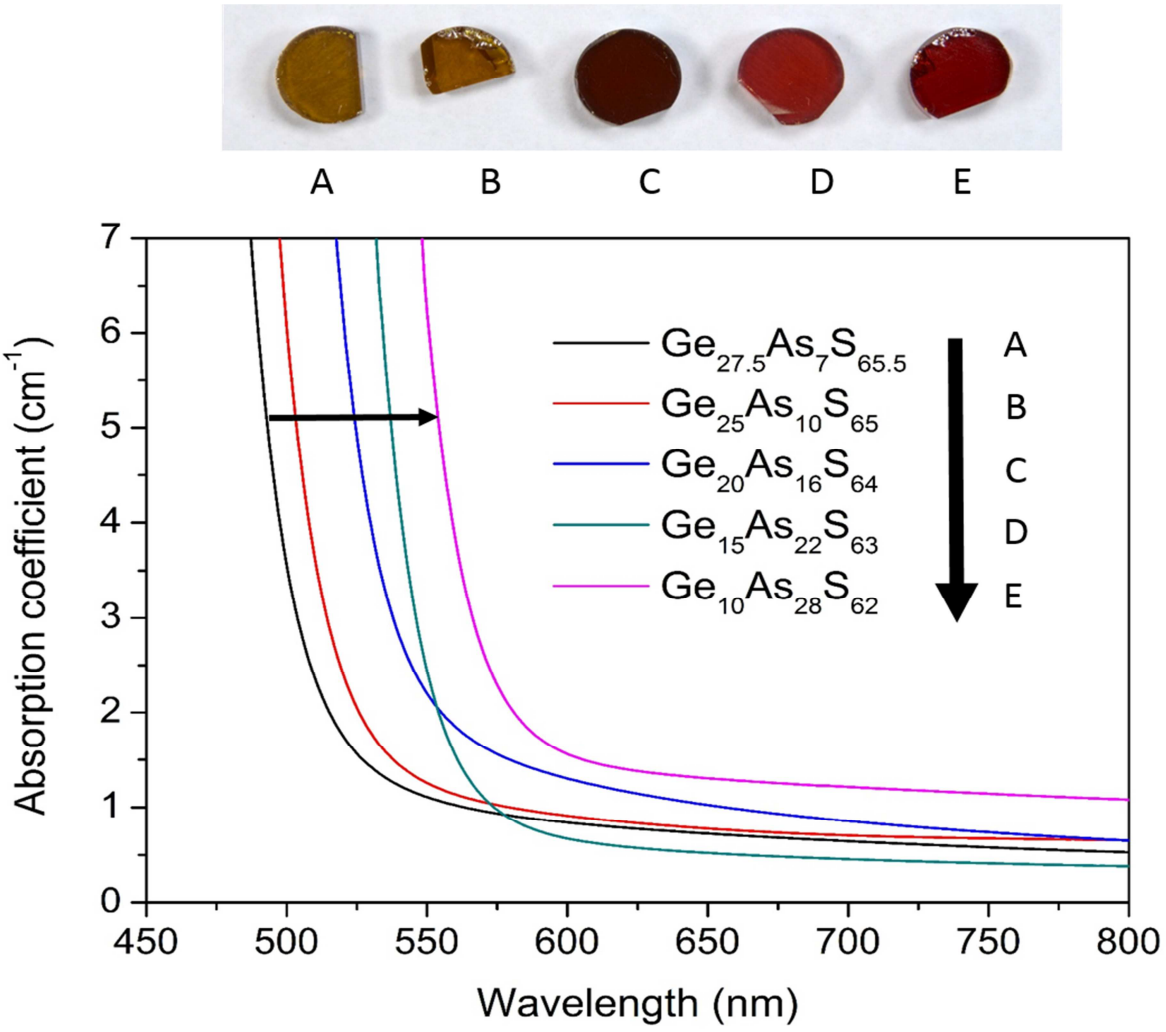

Figure 3: Absorption coefficient in the visible between 500-800 nm of Ge-As-S glasses along the $(GeS_2)_x$—$(As_2S_3)_{100-x}$ composition line

On the other hand, as can be observed in Figure 4, there is no significant change in the multiphonon absorption cut-off around 1000-833 cm^{-1} when germanium was replaced by arsenic. The multiphonon limit is indeed characterized by broad intrinsic absorption bands due to S-S (980 cm^{-1}), $GeS_{4/2}$ (833 cm^{-}

[1]) and $AsS_{3/2}$ (990 cm^{-1}) [20]. However, we can observe the difference in the background absorption depending on the glass compositions. This is due to the fact that their linear refractive indices are different and we did not proceed to a correction of Fresnel reflections. It can be due also to the presence of micro-inhomogeneities in the glass matrix which are relied to impurities. The refractive index depends on the polarizability of the atoms, so the substitution of sulfur by the metalloid elements which are more polarizable induce an increase of the refractive index. Therefore, this explain why the glass $Ge_{30}As_{25}S_{55}$ has a higher background loss. Likewise, we can see that Ge-As-S glasses exhibit extrinsic absorption bands relied to hydrogen or oxygen impurities. As commercial precursors have been used without any specific purifications, many absorption bands have been observed especially due to impurities such as S-H (2500 cm^{-1}), OH_2 (3575, 1585 cm^{-1}), OH^- (3425cm^{-1}), S-OH^- (3225 cm^{-1}), SH_2 (2320 cm^{-1}), Ge-H (2040 cm^{-1}), As-O (1120 cm^{-1}), S-S (1316 cm^{-1}), CS_2 (1510 cm^{-1}) and Ge-O (1265 cm^{-1}) [20,21].

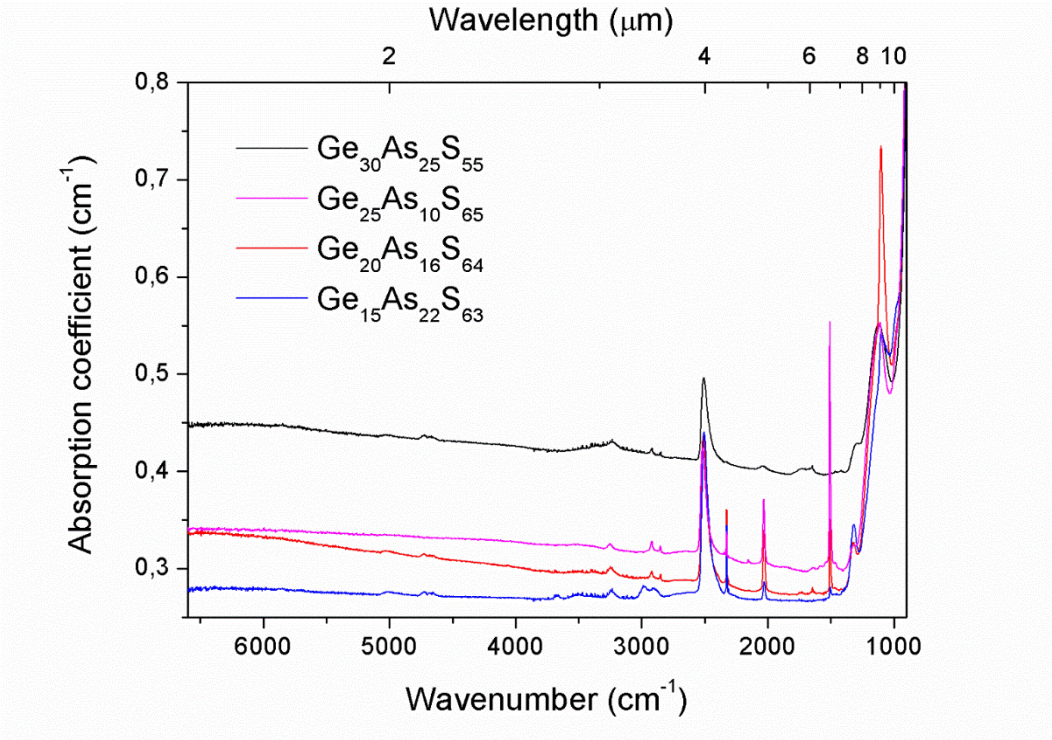

Figure 4: IR absorption coefficient of four different unpurified Ge-As-S glasses between 6600 and 900 cm^{-1}.

Optical fibers

In the first part of this work we performed a thermal study of the different glass compositions. This allowed us to obtain an important thermal properties such as the theoretical drawing temperature or the viscous flow activation energy, which are of great on interest for drawing tests. We were able then to test the stretching into fibers for all the samples except for the $Ge_{15}As_{30}S_{55}$ due to the presence of a crystallization during the viscosity measurement. By taking account of the theoretical drawing temperatures we were able to start fiber drawing experiments around to the real drawing temperature and limits the risk of crystallization. Moreover, having an idea of the viscosity evolution as function of temperature facilitate the drawing tests. Particularly for the compositions with high viscous flow activation energy, as their viscosity could decrease drastically within a small range of temperature and became rather liquid rapidly. The results of the drawing tests are presented in Figure 5. The drawn compositions are presented by black stars, while the red triangles corresponds to compositions which were crystallized. Taking account of the drawing results obtained by T. Kanamori et al. [22] on binary As-S and Ge-S systems (domains delimited by the blue stars) by using the same preform-to-fiber drawing method, we were able to depict a fiber drawing domain inside the glass forming region. Along the $(GeS_2)_x$—$(As_2S_3)_{100-x}$ composition line, we can see that the drawing limit is located between the two compositions $Ge_{27.5}As_7S_{65.5}$ and $Ge_{25}As_{10}S_{65}$. It is well known that GeS_2 glasses are difficult to obtain and present a clear tendency for crystallization, which explain why GeS_2 glass fiber has never been obtained. It is then normal that increasing GeS_2 content until twelve molar percent in the pseudo-binary system, leads to the crystallization of the preform during drawing test. Moreover, one can see that for a

constant Ge/As ratio of 3.93 (arsenic concentration close to 7% around the $(GeS_2)_x$—$(As_2S_3)_{100-x}$ composition line) the tendency for crystallization is more pronounced for composition having an excess of germanium.

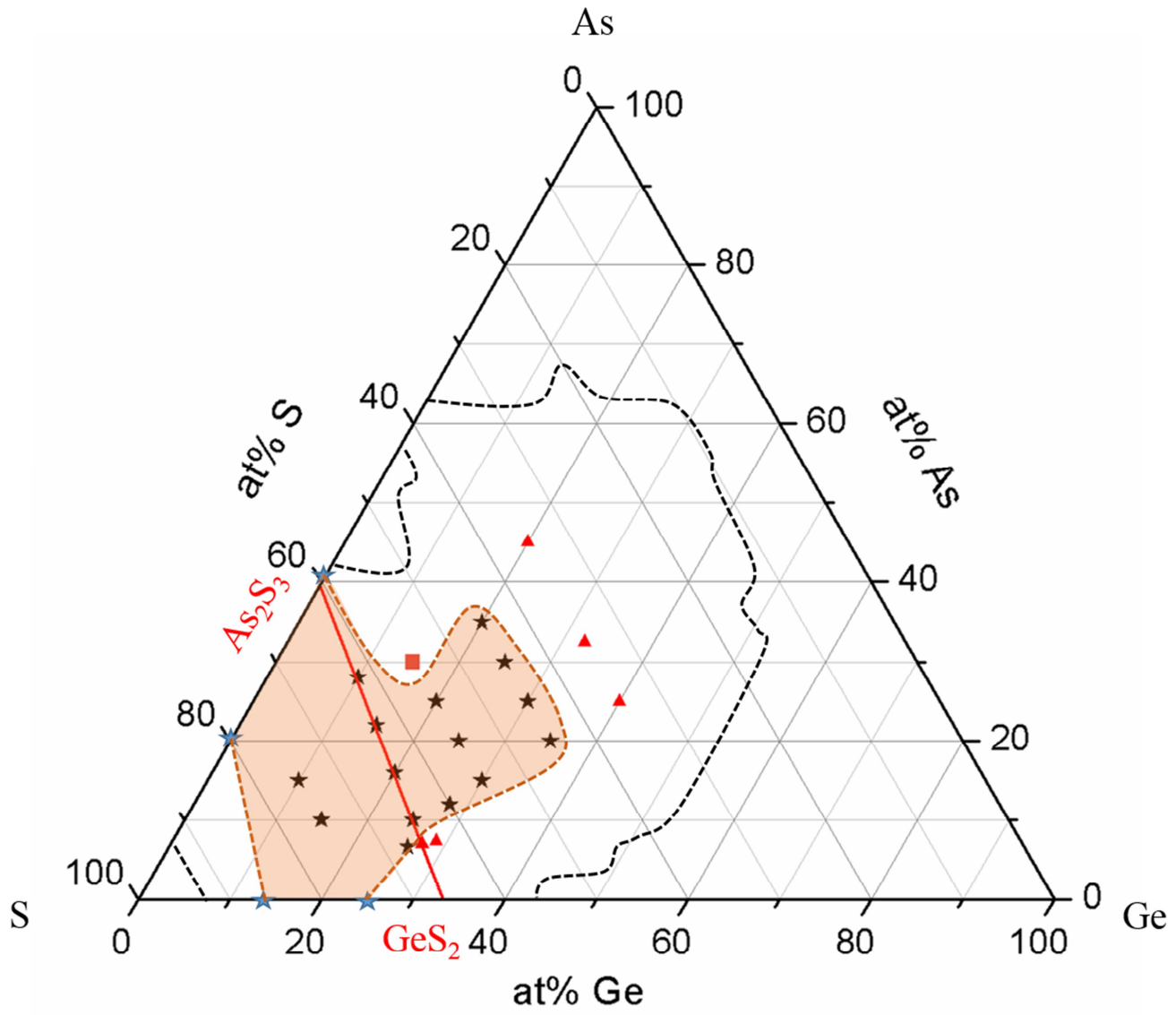

Figure 5: Ge-As-S ternary diagram with (- - -) representing the glass forming region (from Musgraves et al. [5] **) and (- - -) the fiber drawing region. Black stars represents Ge-As-S compositions that could be drawn, blue stars are the compositions delimitating the drawing region between As-S and Ge-S binary systems (from** [22]**). Red triangles characterizes the compositions**

crystallized during the drawing procedure, while orange squares corresponds to the $Ge_{15}As_{30}S_{55}$ composition which have been crystallized during viscosity measurement.

Also we can observe that decreasing the sulfur content under a limit of 45% leads to the crystallization of the preform. At such a low content of sulfur, the links between atoms are essentially dominated by metal bonds, which are less directional and hence lead to an under constrain network, despite the high MCN values. If the bonds are metallic, this turn into a network were the atoms can rearranged more easily and *i.e* to a system more favorable to crystallization. In addition it has to be mentioned that for all the compositions inside the fiber drawing region we were able to deposit a polymer coating, revealing a relatively good mechanical stability. Moreover, using optical microscope, no visible crystallization have been observed on the surface of the fibers.

After drawing, we performed attenuation loss measurement on the obtained fibers. Though the loss are high the fiber was well transmitting in this range of wavelength and one can observe the extrinsic absorption bands due to S-H and O-H at 4.0 µm (2500 cm^{-1}) and 2.92 µm (3425 cm^{-1}) respectively [20]. The losses are due to the use of unpurified raw materials as well as the type of used fiber which was a single index. We remind that the main objective of this work is to explore the possibility to obtain a new optical fiber in Ge-As-S system, so efforts were not been focused on the specific purification. Table 2 resume the attenuation results for some compositions at 1310 and 1550 nm wavelengths. However, using a purification process of the elements and choosing a core/clad fiber instead of single index, we could obtain lower values of losses.

Table 2: Attenuation losses of optical fibers at 1310 and 1550 nm wavelengths using the cut-back technique

	Glass compositions	Loss(dB/m) ± 0.1
@ 1310 nm	$Ge_{28}As_{12}S_{60}$	12.3
	$Ge_{25}As_{10}S_{65}$	12.8
	$Ge_{20}As_{25}S_{55}$	8.4
@1550 nm	$Ge_{15}As_{22}S_{63}$	15.6
	$Ge_{25}As_{30}S_{45}$	24.2

Conclusion

A complete analysis of thermal and physical properties in the Ge-As-S glass system is reported. A particular attention has been paid on TMA and viscosity measurements, and we have been able to measure the values of thermal expansion coefficient, viscous flow activation energy and theoretical drawing temperature except for the two compositions ($Ge_{40}As_{25}S_{35}$ and $Ge_{15}As_{30}S_{55}$). The measured values are in accordance with the previous work reported by B.G. Aitken and C.W. Ponader. The knowledge of these values enabled us to explore the drawing capability of all the glass samples covering wide area of Ge-As-S glass forming region. We showed that it was possible to obtain single index polymer coated optical fibers on a wide range of composition using the classical preform to fiber drawing technique. From the results we were able to depict for the first time a fiber drawing domain inside the Ge-As-S ternary system. The attenuation losses measured at 1310 nm was ranging between 8.4 and 12.3 dB/m. Although this value is high, this is due to the single index geometry of the fibers and the low purity of the raw elements used for the glass synthesis. The wide range of properties of this system combined to his large fiber drawing region reveal an unexplored potential for this ternary system as IR optical fiber or multimaterial fibers.

Acknowledgments

This study has been carried out with financial support from the French Aquitaine region [Grant 2015-1R10205] and by the Canadian Excellence Research Chair program (CERC) in Photonics Innovations. This work has been done in the frame of "the Investments for the future" Programme IdEx Bordeaux-LAPHIA (ANR-10-IDEX-03-02). The authors are also grateful to the Natural Sciences and Engineering Research Council of Canada (NSERC), the Fonds de Recherche Québecois sur la Nature et les Technologies (FRQNT) and the Canadian Foundation for Innovation (CFI) for their financial support.

References

[1] B.J. Eggleton, B. Luther-Davies, K. Richardson, Chalcogenide photonics, Nat. Photonics. 5 (2011) 141–148. doi:10.1038/nphoton.2011.309.

[2] T. Sorokina, K.L. Vodopyanov, Solid-State Mid-Infrared Laser Sources, Berlin, 2003.

[3] B. Molocher, Countermeasure laser development, Proc. SPIE. 5989 (2005) 1–10. doi:10.1117/12.638186.

[4] G.E. Snopatin, V.S. Shiryaev, V.G. Plotnichenko, E.M. Dianov, M.F. Churbanov, High-purity chalcogenide glasses for fiber optics, Inorg. Mater. 45 (2009) 1439–1460. doi:10.1134/S0020168509130019.

[5] J.D. Musgraves, P. Wachtel, B. Gleason, K. Richardson, Raman spectroscopic analysis of the Ge – As – S chalcogenide glass-forming system, J. Non. Cryst. Solids. 386 (2014) 61–66. doi:10.1016/j.jnoncrysol.2013.11.031.

[6] K. Palanjyan, Study of Photoinduced Anisotropy in Chalcogenide Ge-As-S Thin Films, Université Laval, 2015.

[7] B.G. Aitken, C.W. Ponader, Physical properties and Raman spectroscopy of GeAs sulphide glasses, Jounal of Non-Crystalline Solids. 257 (1999) 143–148.

[8] B.G. Aitken, C.W. Ponader, Property extrema in GeAs sulphide glasses, J. Non Cryst. Solids. 274 (2000) 124–130.

[9] J. Kobelke, J. Kirchhof, M. Sche, A. Schwuchow, Chalcogenide glass single mode fibres - preparation and properties, Jounal of Non-Crystalline Solids. 257 (1999) 226–231.

[10] V.G. Plotnichenko, D. V Philippovskiy, V.O. Sokolov, M. V Sukhanov, A.P. Velmuzhov, M.F. Churbanov, E.M. Dianov, Infrared luminescence in Bi-doped Ge–S and As–Ge–S chalcogenide glasses and fibers, Opt. Mater. Express. 4 (2014) 366–374. doi:10.1364/OME.4.000366.

[11] G. Tao, H. Ebendorff-Heidepriem, A.M. Stolyarov, S. Danto, J. V. Badding, Y. Fink, J. Ballato, Abouraddy, A. F., Infrared fibers, Adv. Opt. Photonics. 7 (2015) 379–458. doi:10.1364/AOP.

[12] K. Schuster, S. Unger, C. Aichele, F. Lindner, S. Grimm, Material and technology trends in fiber optics, Adv. Opt. Technol. 3 (2014) 447–468. doi:10.1515/aot-2014-0010.

[13] M. Chazot, M. El Amraoui, S. Morency, Y. Messaddeq, V. Rodriguez, Investigation of the drawing region in the production of Ge-S-I optical fibers for infrared applications, J. Non. Cryst. Solids. 476 (2017) 137–143. doi:10.1016/j.jnoncrysol.2017.09.037.

[14] Y. Luo, Comprehensive Handbook of Chemical Bond Energies, Boca Raton, 2007.

[15] I. Avramov, Viscosity activation energy, Phys. Chem. Glas. Eur. J. Glas. Sci. Technol. B. 48 (2007) 61–63.

[16] M.F. Thorpe, Continuous deformation in random network, J. Non Cryst. Solids. 57 (1983) 355–370.

[17] J.C. Phillips, Topology of covalent non-crystalline solids I: short-range order in chalcogenide alloys, J. Non. Cryst. Solids. 34 (1979) 153–181. doi:10.1016/0022-3093(81)90172-1.

[18] P.M. Nikolic, Z. V. Popovic, Some optical properties of GeS 2 single crystals, J. Phys. C Solid State Phys. 12 (1979) 2–8.

[19] M.S. Lovu, S.D. Shutov, A.M. Andriesh, E.I. Kamitsos, C.P.E. Varsamis, D. Furniss, A.B. Seddon, M. Popescu, Spectroscopic Studies of Bulk As2S3 Glasses and Amorphous Films Doped with Dy, Sm and Mn, J. Optoelectron. Adv. Mater. 3 (2001) 443–454.

[20] V.F. Kokorina, Optical properties of chalcogenide glasses, in: Glas. Infrared Opt., CRC Press, 1996: pp. 75–96.

[21] V. Shiryaev, M. Churbanov, Preparation of high-purity chalcogenide glasses, in: Chalcogenide Glas. Prep. Prop. Appl., Woodhead Publishing Series, 2014: pp. 3–32.

[22] T. Kanamori, Y. Terunuma, S. Takahashi, T. Miyashita, Chalcogenide Glass Fibers for Mid-Infrared Transmission, J. Light. Technol. 2 (1984) 607–613. doi:10.1109/JLT.1984.1073657.